RESEARCH PAPER

PCCP
www.rsc.org/pccp

Computational studies of elementary steps relating to boron doping during diamond chemical vapour deposition

Andrew Cheesman, Jeremy N. Harvey and Michael N. R. Ashfold*

School of Chemistry, University of Bristol, Cantock's Close, Bristol, UK. E-mail: mike.ashfold@bristol.ac.uk

Received 13th December 2004, Accepted 24th January 2005
First published as an Advance Article on the web 15th February 2005

Density functional theory-based electronic structure computations on small models of the diamond {100} surface have enabled prediction of the energetics and activation parameters of a number of plausible mechanistic steps for boron incorporation into, and boron loss from, the growing diamond surface. Initial proving calculations for the carbon-only case show, as in previous work, that the rate-limiting step for diamond growth involves opening of a five-membered ring species, and subsequent closure to form six-membered rings as in bulk diamond. The five-membered ring intermediate arises following 2×1 reconstruction of the {100} surface, or at steps on the {111} surface. Diamond growth arises as a result of successful competition between the ring-opening step and a two-carbon loss step, both of which involve significant activation barriers. In the boron case, we find that BH_x ($x = 0$–3) species can all bind to radical sites on the diamond {100} surface to form stable adducts. Interconversion between the surface bound BH_x species is facile at the H and H_2 number densities and temperatures typical for diamond CVD conditions. B incorporation can occur by a ring expansion mechanism, as in the all-carbon case, and by direct insertion of surface bound BH (and B) species into the C–C bond on the diamond {100} surface. BH_x loss processes identified include release of surface bound BH_3 and/or CH_2BH species into the gas phase. Both B incorporation into, and B loss from, the diamond {100} surface are deduced to be significantly less energy demanding than the corresponding carbon addition and loss processes.

Introduction

Most high quality diamond growth by chemical vapour deposition (CVD) methods involves microwave plasma activation of a hydrocarbon–hydrogen gas mixture (typically 1% CH_4 in H_2) and subsequent deposition onto a hot (*ca.* 800 °C) substrate.[1] An important feature of such plasmas is the high number density of both H atoms and CH_3 (which can typically approach *ca.* 10^{16} cm^{-3} and *ca.* 10^{14} cm^{-3}, respectively). The chemical transformations occurring in such plasmas are dominated by H atom abstraction reactions. These are responsible for generating the gas phase radical species necessary for diamond growth:

$$CH_y + H \leftrightarrow CH_{y-1} + H_2, \text{ where } y = 4 - 1 \qquad (1)$$

H atoms are also vital for forming radical sites on the growing diamond surface, and play a crucial role in etching any non-diamond growth. Diamond growth can begin by CH_3 radical incorporation at a surface radical site.

The {100} surface of diamond has a well known visible 2×1 reconstruction[2] that is driven by steric interactions between H atoms on neighbouring surface carbon atoms and results in formation of a C–C bond in the (100) plane together with loss of molecular hydrogen.[3]

Fig. 1 shows the accepted mechanism for carbon inclusion into this surface. The process is initiated by hydrogen abstraction from a pendant CH_3 radical (*i.e.* C → D in Fig. 1). The surface bound CH_2 then incorporates into the diamond structure *via* a ring opening mechanism (D → E → F) rather than by direct insertion of CH_2 into the C–C bond.[4,5] An alternative process, involving CH_3 radical addition to a pendant CH_2, can lead to the formation of surface bound alkyl chains. Such processes are suppressed under typical diamond CVD conditions, however, by so-called β-scission reactions. Hydrogen abstraction from the β-carbon leads to formation of an unsaturated radical species, which dissociates to form a gas phase species (*e.g.* ethene) and a surface radical site—thereby preventing incorporation of longer alkyl chains into the growing diamond surface.

Addition of trace amounts of a suitable boron-containing precursor to the process gas mixture enables deposition of doped material, in which B atoms have incorporated into both the diamond {100} and {111} surfaces. The elementary steps leading to B incorporation are not well characterised, however. Boron incorporation in diamond creates a (shallow) p-type semiconductor.[6] Sources used for boron inclusion during diamond CVD include diborane, trimethylboron and triethylboron.[7–10] Several studies have highlighted the preferential incorporation of boron in (111) growth sectors.[9,11,12] The advent of B doped CVD diamond has led to the development of intrinsic devices,[13] electrochemical detectors,[12,14] and when combined with P (n-type) doped diamond, UV light sources.[15] Much further interest has been stimulated by recent reports of n-type electrical conductivity from deuterated (100) B-doped diamond layers.[16] Theory has thus far failed to validate initial suggestions that such conductivity might be associated with boron–deuterium complex defects within the diamond lattice.[17]

Thermochemical modelling of dilute B_2H_6/H_2 gas mixtures in the presence of H atoms at gas temperatures relevant to CVD diamond growth indicates formation of a range of BH_x, $x = 0$–3 species, with B and BH_3 being the most abundant.[18,19] Harris *et al.*[20,21] have calculated reaction mechanisms and rates for hydrogen abstraction from, and insertions into, BH_x species.

$$BH_x + H \leftrightarrow BH_{x+1} \leftrightarrow BH_{x-1} + H_2, \text{ where } x = 3 - 1 \quad (2)$$

Reactions (2) can occur either through a low energy BH_{x+1} intermediate formed from coordination of the atomic hydrogen with the valence p orbital on the boron atom, as shown, or

DOI: 10.1039/b418664h

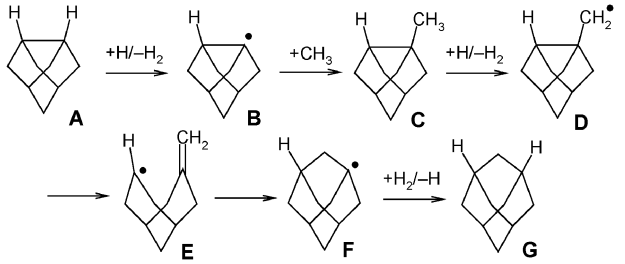

Fig. 1 Mechanism for surface activation and carbon incorporation into the diamond (100) surface.

by direct abstraction. Companion experimental and modelling studies of gas phase B atom number density distributions in hot filament activated B_2H_6/H_2 and $B_2H_6/CH_4/H_2$ gas mixtures, and their variation with process conditions will be reported elsewhere.[18]

Computational methods have played an important role in helping to understand the gas-surface reaction mechanisms involved in diamond CVD,[3,5] but have not yet made many contributions to understanding the specific mechanisms of dopant incorporation.[22] The aims of the preliminary theoretical investigations reported here were to identify likely B containing growth species and to investigate plausible mechanisms both for B incorporation into, and B loss from the {100} surface during diamond CVD.

Computational details

As in previous modelling studies of the carbon growth step on a diamond (100) surface with 2 × 1 reconstruction,[5] our calculations are based on a C_9H_{14} cluster (structure A in Fig. 1). Preliminary studies employing a larger model of the diamond surface, and a hybrid DFT/molecular mechanics (MM) procedure, suggest that the energies and structures computed here are similar to those expected for the full surface, encouraging the view that the present conclusions should be sound. Potential energy minima and transition states for the present cluster model were fully optimized using the standard B3LYP functional together with the 6-31G* basis set within the Gaussian 03 program package.[23] Vibrational frequencies were computed to confirm the nature of the stationary points as either minima (all real frequencies) or transition states (one imaginary frequency). Single-point B3LYP energies were computed at the B3LYP/6-31G* geometries using the larger 6-311+G(2df,p) basis. All reported energy differences (ΔE) and activation energies (E_a) are based on B3LYP/6-311+G(2df,p) energies with the B3LYP/6-31G* geometries and zero-point energy corrections. Based on the computed vibrational frequencies and rotational constants, rigid rotor–harmonic oscillator statistical mechanics was carried out at various temperatures using Gaussian 03 to generate free energy thermal corrections to the B3LYP/6-311+G(2df,p) energies. The standard free energies of activation and free energies of reaction reported later in this work are derived in this way.

The computed ΔE and ΔG values, and the temperature dependence of the latter, are affected by various errors due to the use of approximate density functional theory (B3LYP), the use of a small model cluster for the diamond surface, and the use of the rigid rotor–harmonic oscillator approximation for computation of thermal effects. Taken together, these errors could, in principle, lead to a total error on relative energies of well over 50 kJ mol^{-1}. However, the error is unlikely to be this large in all cases, and some error cancellation is expected. As discussed later, benchmarking CCSD(T) calculations using the much larger cc-pVQZ basis have been carried out (at the B3LYP/6-31G* geometries) for one simple case, to calibrate the B3LYP method. These latter calculations were carried out using the MOLPRO program package.[24]

Results and discussion

A. Boron addition to the cluster surface

Hydrogen abstraction from the diamond (100) surface (*i.e.* process A → B in Fig. 1) was calculated to be virtually thermoneutral, ($\Delta E = -16.5$ kJ mol^{-1}) and to have a low activation barrier ($E_a = 16.2$ kJ mol^{-1}), in good agreement with previous calculated values.[5]

Addition of the various gaseous BH_x ($x = 0$–3) species to a surface site radical was then modelled. Strong B–C bonds result for $x = 0$, 1 or 2 ($\Delta E = -363.0$, -368.9 and -408.3 kJ mol^{-1}, respectively), comparable to the energy release upon C–C bond formation when CH_3 adds to the same surface site ($\Delta E = -353.8$ kJ mol^{-1}). Interestingly, the optimized structures show that the adsorbed boron atom aligns its empty valence p-orbital parallel to the strained (100) C–C bond, presumably due to a stabilizing hyperconjugation interaction. BH_3 addition to the surface is calculated to be much less exothermic ($\Delta E = -46.9$ kJ mol^{-1}). The geometry adopted by the surface-bound BH_3 is not tetrahedral, but a mildly distorted trigonal configuration, with a weak interaction of the boron atom with the diamond surface radical site through the unoccupied p orbital.

Hydrogen abstraction from surface bound BH_x, $x = 1$, 2, species occurs *via* analogues of reaction (2). As in the purely gas phase case,[20,21] abstraction may occur either directly, or *via* a sequential mechanism in which H atom addition is followed by loss of H_2. In the case of surface bound BH_2, H atom loss *via* the sequential mechanism involves an initial exothermic ($\Delta E = -68.4$ kJ mol^{-1}) addition to form surface bound BH_3, followed by endothermic loss of H_2 ($\Delta E = 56.0$ kJ mol^{-1}). The overall conversion is mildly exothermic ($\Delta E = -12.4$ kJ mol^{-1}). We have checked that hydrogen loss has no barrier above the endothermicity by carrying out a set of constrained geometry optimizations with increasing B–H_2 distances; this gives a smoothly increasing curve tending towards the energy of separated surface bound BH and H_2.

Abstraction from surface bound BH is much more exothermic ($\Delta E = -118.4$ kJ mol^{-1}). We have not explicitly located transition states for either the direct or the indirect abstraction processes but, by analogy with the reaction of H atoms with gas-phase BH_2,[20,21] neither pathway is expected to involve a significant energy barrier. Inter-conversion between surface-bound B, BH and BH_2 is thus expected to be facile in the presence of H atom number densities and at temperatures prevailing in successful diamond CVD.

B. Boron insertion into the diamond surface

Once a BH_x species has been attached to the surface, it then needs to insert into a surface C–C bond. This requires that the reconstructed (100) C–C bond breaks, and that a new B–C bond is formed. Energetically feasible insertion pathways for surface bound BH and B species have been identified, and are described in this section.

As shown in Fig. 1, the mechanism for the analogous carbon insertion reaction, starting from the surface bound CH_2 radical (D), involves two steps: C–C bond cleavage, to form an unsaturated –CH=CH_2 fragment (E), followed by cyclization to form the carbon-inserted isomer (F). The transition states (TSs) for these two steps lie fairly close in energy, at 43.2 and 57.2 kJ mol^{-1} above the starting radical. The geometry and relative energy of these two transition states are similar to those reported previously.[5] A transition state for direct insertion was also located in this previous work,[5] but was found to lie at much higher energy (*ca.* 200 kJ mol^{-1}). Although the barriers involved are fairly low, the ring-opening and closing sequence has been suggested to be rate-limiting for diamond growth.[5]

We have located transition states corresponding to analogous indirect and direct insertion of a surface bound BH

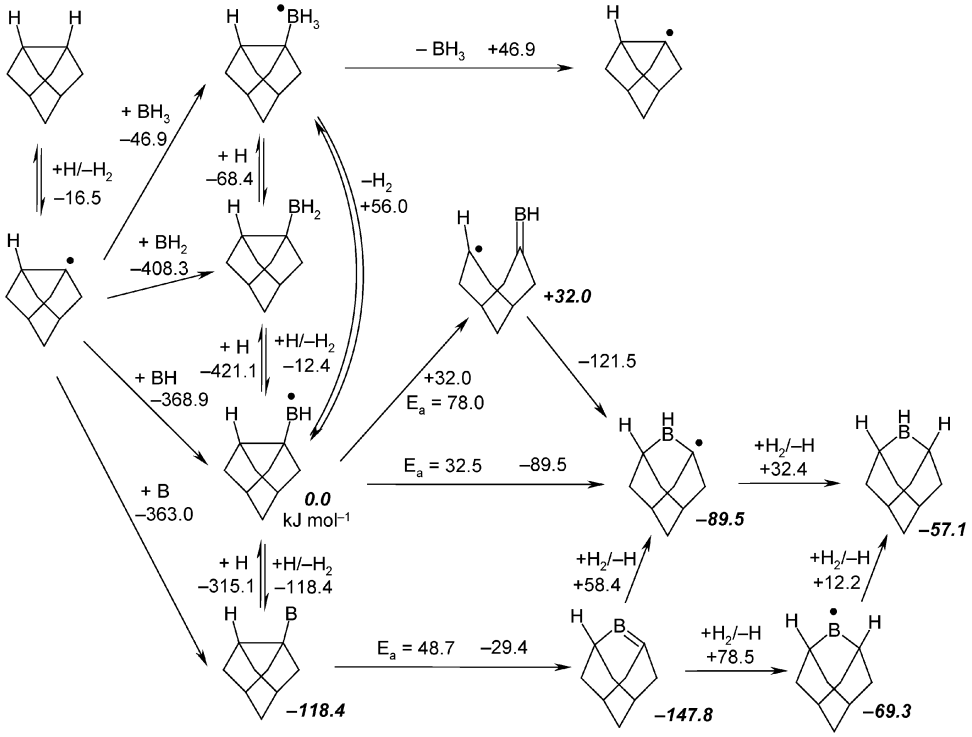

Fig. 2 Overview of the reaction pathways for BH_x addition to, incorporation into, and loss from, the diamond (100) surface. Numbers beneath the various structures (in bold italics) indicate their calculated energies (in kJ mol^{-1}) relative to the surface bound BH species. Reaction energies and activation energies are shown in normal script next to the corresponding arrow.

radical into the adjacent C–C bond (Fig. 2). In stark contrast to the carbon case, the direct mechanism with boron is found to be significantly more favourable ($E_a = 32.5$ kJ mol^{-1}, $\Delta E = -89.5$ kJ mol^{-1}) than the indirect mechanism, which involves ring-opening and closing barriers lying, respectively 78.0 and 70.3 kJ mol^{-1} above the starting species. The low relative energy of the direct pathway is due to the availability of one empty (as well as the singly occupied) valence p orbital on boron which can interact directly with the second carbon atom, thereby enabling simultaneous bond-breaking and formation. (Note that in the related all carbon sequence (Fig. 1, steps D → E → F) there is no analogous vacant p orbital. Both the indirect and direct BH insertion reaction mechanisms in Fig. 2 lead to the same species; further H atom addition (or abstraction of H from gas-phase H_2) will terminate the remaining surface radical site and conclude the B insertion process. As shown in Fig. 2, there is also a direct insertion process starting from a surface bound B atom. This too has a low activation barrier ($E_a = 48.7$ kJ mol^{-1}), and is exothermic ($\Delta E = -29.4$ kJ mol^{-1}). From the inserted species, two consecutive H atom additions result in the same stabilised product as that obtained when starting from the surface bound BH species. Clearly, the barrier for this step is sufficiently low to encourage the view that it too may play a role in the growth of B-doped diamond.

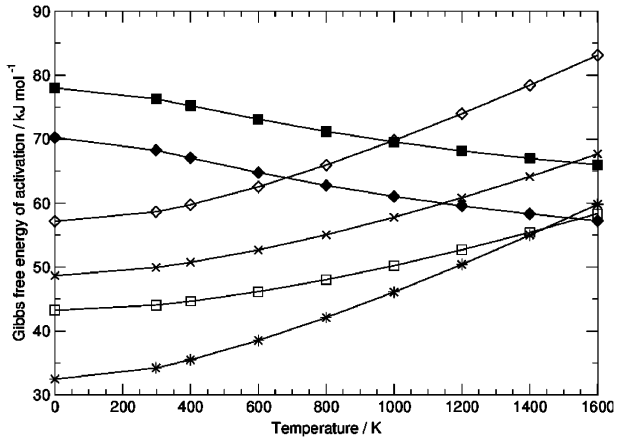

Fig. 3 Calculated temperature dependent free energies of activation for selected key steps in the incorporation of BH_x species into a diamond (100) surface: × insertion of B; * direct insertion of BH; ■ ring opening for BH insertion; ◆ ring closing for BH insertion. Also shown, for comparison, are the corresponding free energies for: □ ring opening for CH_2 insertion; ◇ ring closing for CH_2 insertion.

Fig. 3 shows the temperature dependence of the free energies of activation for the key TSs involved in these B and BH insertion processes, calculated relative to the respective surface bound activated species. Direct insertion of BH is calculated to involve the transition state of lowest free energy at all temperatures <1500 K. Also shown, for comparison, are the corresponding temperature dependent activation free energies for carbon insertion starting from the surface bound CH_2 species (structure D in Fig. 1). As Fig. 3 shows, the transition states involved in all of the ring opening and closing reactions, for both boron and carbon, are calculated to lie higher in free energy than that for the direct BH insertion process.

The present mechanism leads to incorporation of a trivalent boron species into the diamond surface. This can then undergo hydrogen addition, formation of a new 2 × 1 reconstructed C–B bond with an adjacent CH_2 group, and further addition of carbon to lead ultimately to a substitutional, tetravalent boron atom in the diamond bulk.[17] We have not yet investigated these steps, which are assumed to occur in a similar fashion to the related all-carbon chemistry.

C. Loss processes from the diamond surface

As shown above, boron in the form of B, BH or BH_2 can attach readily to activated surface sites on a diamond (100) surface, and inter-conversion between surface-bound B, BH and BH_2 species is likely to be facile under the conditions typically used for diamond CVD. Subsequent boron insertion (as BH or B) involves a significantly lower energy transition state than those involved in CH_2 insertion. Diamond CVD is a dynamic process involving simultaneous growth and etching

(loss) steps. The extent of boron incorporation into CVD diamond depends not only on the activation barriers for the insertion steps, discussed in the previous section, but also on the relative rates of carbon and boron loss; these also need to be considered.

It is reasonable to assume that loss is unlikely to occur once boron or carbon has been inserted into the C–C bond of a (100) surface. Thus the key intermediates in modelling possible loss processes are the surface bound BH_x and CH_x species. Direct unimolecular carbon loss mechanisms for these species involve breaking a strong C–C bond and are thereby very endothermic and unfavourable. Abstraction of methane by reaction of an H atom with surface bound CH_3 involves a very high activation barrier, and can also be discounted. Instead, the energetically least demanding way to remove carbon from the surface is to add a second carbon. This so-called β-scission mechanism is shown in Fig. 4a. It involves CH_3 addition to structure (D) in Fig. 1, to form a pendant ethyl radical. C–H bond activation by hydrogen atoms resulting in a surface bound CH_2CH_2 species, which can dissociate into the gas phase in a process that is far less endothermic than the direct C–C bond cleavage in surface-bound CH_3. The final loss step is only endothermic by 172.6 kJ mol^{-1}, and is entropically favourable. As shown in Fig. 5, the free energy for loss of ethene *via* the β-scission step is calculated to become favourable at higher temperatures (>1100 K). Note that we have not computed the free energy of activation for this step or for the other loss processes, but as these are endothermic reactions with no energy barriers above the endothermicity, the free energy of reaction should be very similar to the free energy of activation.

We have identified a greater variety of mechanisms that could contribute to loss of surface bound boron. First of all, in analogy to the all-carbon chemistry, there are two distinct β-scission routes, shown in Fig. 4, leading to loss of boron in the form of gas-phase CH_2BH. The first process is the more important one, as it leads to cleavage of the surface C–B bond. The alternative process, shown in Fig. 4c, is less relevant as it only leads to C–C bond breaking. It is interesting to observe that the final bond-breaking step is significantly more endothermic for step 5b than for the C–C bond breaking steps in 5a and 5c. This can be explained in terms of the stabilization in the precursor radicals: the radical on the terminal CH_2 group in the case of 5b is stabilized by delocalization into the vacant p orbital on boron. There is no such stabilization effect in the other two cases. Boron loss by the reaction shown in Fig. 4b only becomes favourable above 1400 K, so probably does not play a role under CVD conditions.

However, there is another, more favourable, mechanism for loss of surface bound B species. As Fig. 2 showed, hydrogen atom addition to a surface bound BH_2 species yields surface bound BH_3 in an exothermic step ($\Delta E = -68.4$ kJ mol^{-1}). The B–C bond in the latter adduct is rather weak so that BH_3 release into the gas phase ($\Delta E = 46.9$ kJ mol^{-1}) should compete with loss of dihydrogen to give surface bound BH ($\Delta E = 56.0$ kJ mol^{-1}). It is to be noted that due to the many potential errors in our computational approach, it is not possible to conclude that BH_3 loss from the surface is less energetically demanding than H_2 loss from the surface bound BH_3 moiety—only that these two processes are likely to be of comparable energy. To probe this, we have computed more accurate energetics for a simpler model system, $CH_3BH_2 + H \rightarrow$ (a) $CH_3BH_3 \rightarrow$ (b) $CH_3 + BH_3$ or (c) $CH_3BH + H_2$. Intermediate (a) is predicted to have a relative energy of −26.2 kJ mol^{-1} compared to reagents at the same B3LYP level used for our other calculations, and products (b) and (c) have energies relative to CH_3BH_2 and H of, respectively, −10.6 and −15.6 kJ mol^{-1}. These energies are fairly similar for those found at the B3LYP level for the B doped diamond model (−68.4, −21.5, −12.4 kJ mol^{-1}, Fig. 2). The B3LYP results are also in fairly good agreement with the CCSD(T) single point energies which are, respectively, −16.6, −3.6 and −2.9 kJ mol^{-1} for intermediate (a) and products (b) and (c), suggesting that B3LYP is fairly accurate for this system.

Similar processes can lead to C–B bond cleavage starting from other surface-bound boron species. For example, addition of a hydrogen atom to a surface-bound B atom, followed by addition of H_2 and loss of BH_3 provides an easy, low-energy pathway for boron loss. Free energy differences for some of these reactions are shown in Fig. 5. As mentioned above, these are free energies of reaction, not free energies of activation. The latter are difficult to compute for these processes without barriers, but are expected to be similar to the reaction free energies. An additional difficulty for assessing the relative ease of borane loss and incorporation is that it is not easy to define the relevant free energies for the loss processes. For example, the elementary step of borane loss from surface bound BH_3 is not the rate-limiting step for borane loss as the surface bound BH_3 species will only have a very short lifetime following formation by H atom addition to surface bound BH_2, and will rapidly decompose by loss of either H, H_2 or BH_3. No other individual step or combination of steps is obviously rate-limiting, so we show instead in Fig. 5 the standard free energy change associated with a number of relevant transformations. Note that the loss processes themselves are favoured in terms of free energy at most temperatures, but H atom addition to surface bound BH_2, a necessary step before loss can occur, becomes unfavourable at higher temperatures due to entropic factors. Arguably, the most important observation is that the loss chemistry is feasible from all surface-bound boron species at all temperatures.

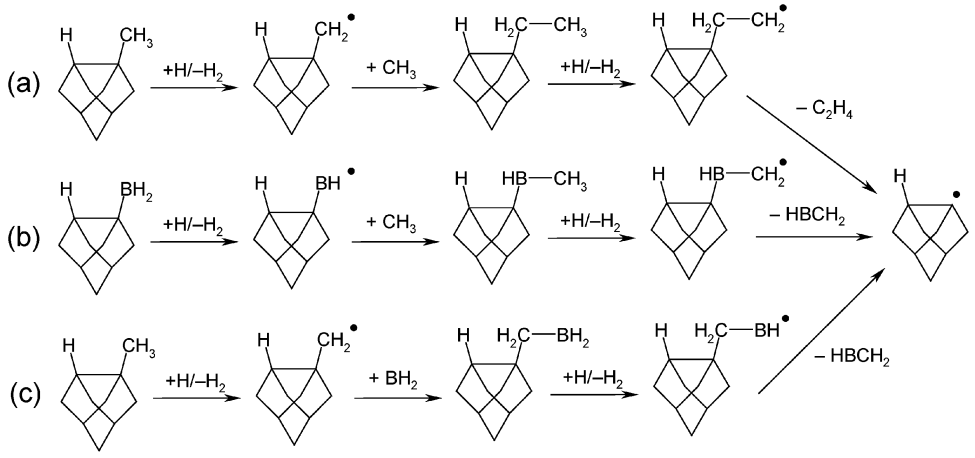

Fig. 4 β-Scission reaction pathways leading to (a) C_2H_4 or (b) and (c) $HBCH_2$ loss from a diamond (100) surface. $HBCH_2$ loss can occur either *via* B–C bond fission (b) or *via* C–C bond fission (c).

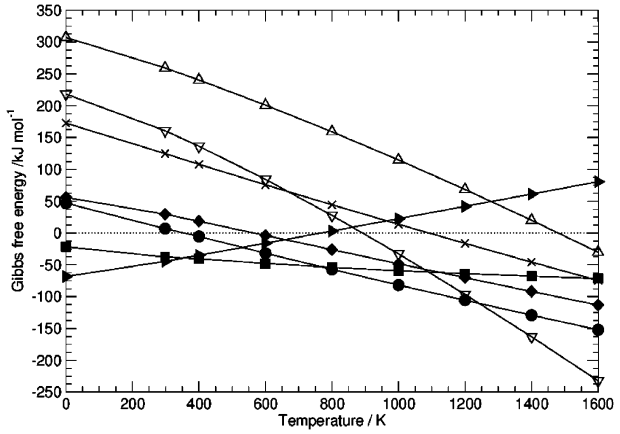

Fig. 5 Calculated temperature dependent free energies of reaction for dissociation processes at a diamond (100) surface. ▶ Surf–BH_2 + H → Surf–BH_3; ■ Surf–BH_2 + H → Surf + BH_3; ● Surf–BH_3 → Surf + BH_3; ◆ Surf–BH_3 → Surf–BH + H_2; × Surf–C_2H_4 → Surf + C_2H_4; ▽ Surf –CH_2BH → Surf + CH_2BH (Fig. 4c); Δ Surf–$BHCH_2$ → Surf + CH_2BH (Fig. 4b).

It is thus clear that BH_3 loss is likely to be easier than carbon loss (in the form of C_2H_4) as it involves only steps with low barriers and low endothermicities. The impact of this on boron incorporation during diamond CVD is hard to assess in the absence of a detailed kinetic model of the gas-phase and surface chemistry, which is beyond the scope of this work. It is already apparent, however, that BH_3 and B atoms are the dominant boron-containing species in the gas phase.[18,20,21] BH_3 addition to an unsaturated surface site on diamond could lead to incorporation provided H_2 loss competes favourably with desorption of borane—the two processes lie close in energy. B atom addition to the surface can certainly lead to incorporation, as surface bound boron itself, or surface bound BH, can undergo relatively easy insertion into the C–C bond. However, low-energy pathways also exist for boron atom desorption.

Conclusions

BH_x ($x = 0$–3) species can bind to radical sites on the diamond {100} surface to form stable adducts. Inter-conversion between the surface bound BH_x species is facile at the H and H_2 number densities and temperatures prevailing in typical diamond CVD conditions. Mechanisms for direct insertion of surface bound BH (and B) species into a growing (100) face of diamond have been identified, as has an alternative ring opening/closing sequence for incorporating BH. This latter process is the boron analogue of the mechanism by which carbon addition into the (100) surface is traditionally envisioned.[5] Direct insertion of BH is calculated to involve the transition state of lowest free energy at all temperatures <1500 K. Several BH_x loss processes from the surface have also been identified. The calculated binding energy of a surface bound BH_3 species is sufficiently weak that direct loss into the gas phase is likely under typical CVD conditions. Boron can also be lost from the surface as, for example, CH_2BH, by a β-scission mechanism. Both B incorporation into, and B loss from, the diamond {100} surface are thus deduced to be more facile than the corresponding carbon addition and loss processes. Estimates of the relevant energetics are a necessary precursor to any more complete description of B incorporation during diamond CVD, even into just the {100} surface, but a full description will eventually require proper simulation of both the gas-surface interactions and the surface-growth kinetics.

The present conclusions are based on computations at the B3LYP level of theory. Test calculations at the CCSD(T) level for an even smaller model system show that the computed B3LYP energetics are fairly reliable. The use of such a small model for the diamond {100} surface is also a cause for concern. However, preliminary work using a much larger model of the diamond surface, together with a hybrid DFT/MM procedure, suggests that the energies and structures computed here are similar to those expected for the full surface, thus encouraging the view that the present conclusions should be reliable.

Acknowledgements

Helpful discussions with Dr J. P. Goss (University of Newcastle-upon-Tyne) are gratefully acknowledged, as is the financial support of EPSRC (in the form of an Advanced Research Fellowship to JNH, and the portfolio award LASER) and Element Six Ltd (Industrial CASE studentship to AC).

References

1 D. G. Goodwin and J. E. Butler, in *Handbook of Industrial Diamonds and Diamond Films*, ed. M. A. Prelas, G. Popovici and L. K. Bigelow, Marcel Dekker Inc., New York, 1998, p. 527, and references therein.
2 K. Bobrov, A. Mayne, G. Comtet, G. Dujardin, L. Hellner and A. Hoffman, *Phys. Rev. B*, 2003, **68**, 195416.
3 D. Huang and M. Frenklach, *J. Phys. Chem.*, 1992, **96**, 1868.
4 B. J. Garrison, E. J. Dawnkaski, D. Srivastava and D. W. Brenner, *Science*, 1992, **255**, 835.
5 J. K. Kang and C. B. Musgrave, *J. Chem. Phys.*, 2000, **113**, 7582.
6 J. F. H. Custers, *Physica (Amsterdam)*, 1952, **18**, 489.
7 Z. Y. Xie, J. H. Edgar, T. L. McCormick and M. V. Sidorov, *Diamond Relat. Mater.*, 1998, **7**, 1357.
8 S. Yamanaka, H. Watanabe, S. Masai, D. Takeuchi, H. Okushi and K. Kajimura, *Jpn. J. Appl. Phys.*, 1998, **37**, L1129.
9 P. Wurzinger, P. Pongratz, P. Hartmann, R. Haubner and B. Lux, *Diamond Relat. Mater.*, 1997, **6**, 763.
10 A. Deneuville, *Semicond. Semimet.*, 2003, **76**, 183.
11 R. Samlenski, C. Haug, R. Brenn, C. Wild, R. Locher and P. Koidl, *Diamond Relat. Mater.*, 1996, **5**, 947.
12 J. Angus, Y. V. Pleskov and S. C. Eaton, *Semicond. Semimet.*, 2004, **77**, 97.
13 J. Isberg, J. Hammersberg, E. Johansson, T. Wikström, D. J. Twitchen, A. J. Whitehead, S. E. Coe and G. A. Scarsbrook, *Science*, 2002, **297**, 1670.
14 M. N. Latto, D. J. Riley and P. W. May, *Diamond Relat. Mater.*, 1999, **9**, 1181.
15 S. Koizumi, K. Watanabe, F. Hasegawa and H. Kanda, *Science*, 2001, **292**, 1899.
16 Z. Teukam, J. Chevallier, C. Saguy, R. Kalish, D. Ballutaud, M. Barbé, F. Jomard, A. Tromson-Carli, C. Cytermann, J. E. Butler, M. Bernard, C. Baron and A. Deneuville, *Nature Mater.*, 2003, **2**, 482.
17 J. P. Goss, P. R. Briddon, S. J. Sque and R. Jones, *Phys. Rev. B*, 2004, **69**, 165215.
18 A. Cheesman, D. M. Comerford, R. S. Sage, D. M. E. Davies, J. A. Smith, M. N. R. Ashfold and Yu. A. Mankelevich, manuscript in preparation.
19 C. L. Yu and S. H. Bauer, *J. Phys. Chem. Ref. Data*, 1998, **27**, 807.
20 S. J. Harris, J. Kiefer, Q. Zhang, A. Schoene and K. W. Lee, *J. Electrochem. Soc.*, 1998, **145**, 3203.
21 H. B. Schlegel, A. G. Baboul and S. J. Harris, *J. Phys. Chem.*, 1996, **100**, 9774.
22 See, however K. Larsson, *Phys. Stat. Sol.*, 2002, **193**, 409, for a study of N, P and S reactions at the diamond surface.
23 M. J. Frisch, G. W. Trucks, H. B. Schlegel, G. E. Scuseria, M. A. Robb, J. R. Cheeseman, J. A. Montgomery Jr, T. Vreven, K. N. Kudin, J. C. Burant, J. M. Millam, S. S. Iyengar, J. Tomasi, V. Barone, B. Mennucci, M. Cossi, G. Scalmani, N. Rega, G. A. Petersson, H. Nakatsuji, M. Hada, M. Ehara, K. Toyota, R. Fukuda, J. Hasegawa, M. Ishida, T. Nakajima, Y. Honda, O. Kitao, H. Nakai, M. Klene, X. Li, J. E. Knox, H. P. Hratchian, J. B. Cross, C. Adamo, J. Jaramillo, R. Gomperts, R. E. Stratmann, O. Yazyev, A. J. Austin, R. Cammi, C. Pomelli, J. W. Ochterski, P. Y. Ayala, K. Morokuma, G. A. Voth, P. Salvador, J. J. Dannenberg, V. G. Zakrzewski, S. Dapprich, A. D. Daniels,

M. C. Strain, O. Farkas, D. K. Malick, A. D. Rabuck, K. Raghavachari, J. B. Foresman, J. V. Ortiz, Q. Cui, A. G. Baboul, S. Clifford, J. Cioslowski, B. B. Stefanov, G. Liu, A. Liashenko, P. Piskorz, I. Komaromi, R. L. Martin, D. J. Fox, T. Keith, M. A. Al-Laham, C. Y. Peng, A. Nanayakkara, M. Challacombe, P. M. W. Gill, B. Johnson, W. Chen, M. W. Wong, C. Gonzalez and J. A. Pople, *GAUSSIAN 03, (Revision B04)*, Gaussian, Inc., Pittsburgh PA, 2003.

24 R. D. Amos, A. Bernhardsson, A. Berning, P. Celani, D. L. Cooper, M. J. O. Deegan, A. J. Dobbyn, F. Eckert, C. Hampel, G. Hetzer, P. J. Knowles, T. Korona, R. Lindh, A. W. Lloyd, S. J. McNicholas, F. R. Manby, W. Meyer, M. E. Mura, A. Nicklass, P. Palmieri, R. Pitzer, G. Rauhut, M. Schütz, U. Schumann, H. Stoll, A. J. Stone, R. Tarroni, T. Thorsteinsson and H.-J. Werner, *MOLPRO, a package of ab initio programs designed by H.-J. Werner and P. J. Knowles, Version 2002.1*, 2002.

